

## Synthesis of alloyed Zn<sub>1-x</sub>Mn<sub>x</sub>S nanowires with completely controlled compositions and tunable bandgaps

Jing Cai<sup>\*a</sup>, Sheng Wang<sup>a</sup>, Kefu Zhu<sup>a</sup>, Yucheng Wu<sup>\*a</sup>, Lizhao Zhou<sup>a</sup>, Yongliang Zhang<sup>a</sup>, Qiang Wu<sup>b</sup>, Xizhang Wang<sup>\*b</sup> and Zheng Hu<sup>b</sup>

**Table S1.** Lattice parameter  $a$  and the  $x$  value of Zn<sub>1-x</sub>Mn<sub>x</sub>S estimated by the Vegard's law.

sample number (#)	Lattice parameter $a$ (Å)	$x$ value
1	3.8174	0
2	3.8333	0.10
3	3.8547	0.23
4	3.8696	0.32
5	3.8948	0.47
6	3.9223	0.64
7	3.9308	0.70
8	3.9535	0.83
9	3.9805	1

The  $a$  values were calculated following the equation S1 below,

$$\text{For } (hk0) \quad a = \frac{\lambda}{\sin\theta} \sqrt{\frac{h^2 + hk + k^2}{3}} \quad (\text{S1})$$

The  $x$  values were calculated following the equation 1 (in the main text). The relationship between  $a$  and  $d_{h00}$  following the equation S2 below,

$$d_{h00}^2 = \frac{3a^2}{4h^2} \quad (\text{S2})$$

**Table S2.** The optical bowing parameters  $b$  of three chalcogenide nanomaterials and their relevant physical chemical parameters

Three chalcogenide nanomaterials	Optical bowing parameter $b$ /eV	Electronegativity <sup>a</sup>			atomic radius (covalent radius) <sup>a</sup> /Å			Lattice constant/Å		
				Difference			Difference			Mismatch/%
Zn <sub>1-x</sub> Mn <sub>x</sub> S nanowires in this study	<b>0.74</b>	Mn: 1.55	Zn: 1.65	<b>0.10</b>	Mn: 1.29	Zn: 1.20	<b>0.09</b>	$a$ of MnS (JCPDS:40-1289): 3.9792	$a$ of ZnS (JCPDS:36-1450): 3.8210	<b>4<sup>b</sup></b>
PbS <sub>x</sub> Se <sub>1-x</sub> nanocrystals <sup>1</sup>	<b>0.19</b>	S: 2.58	Se: 2.55	<b>0.03</b>	S: 1.04	Se: 1.18	<b>0.14</b>			<b>~2<sup>ref.1</sup></b>
ZnSe <sub>x</sub> Te <sub>1-x</sub> nanowires <sup>2</sup>	<b>1.28</b>	Se: 2.55	Te: 2.10	<b>0.45</b>	Se: 1.18	Te: 1.37	<b>0.19</b>	$a$ of ZnSe (JCPDS: 89-2940): 3.996	$a$ of ZnTe (JCPDS: 19-1482): 4.310	<b>8<sup>b</sup></b>

<sup>a</sup>: The data are cited from the ref.<sup>3</sup>

$$= \frac{2|a_A - a_B|}{a_A + a_B} \quad (\text{S3})$$

<sup>b</sup>: The lattice mismatch values are estimated following the equation S3: Mismatch

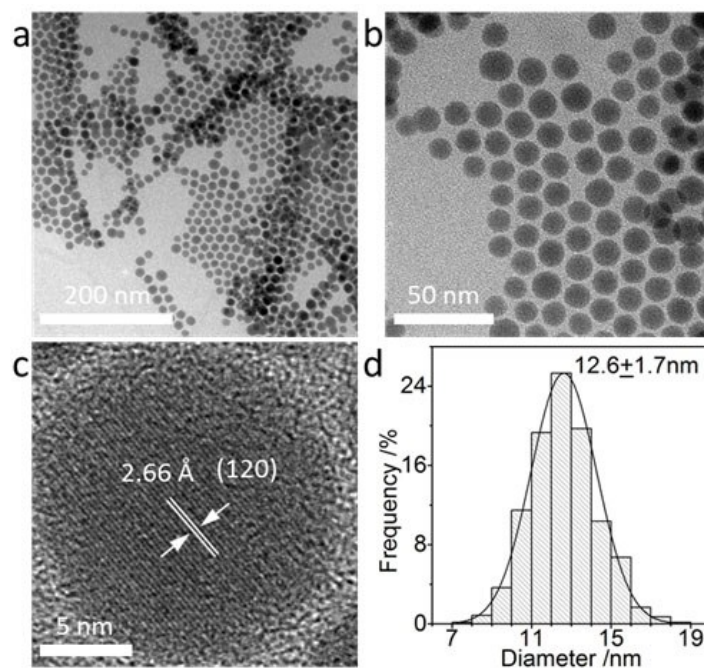


**Fig. S1** (a, b) TEM and (c) HRTEM images of the typical  $\text{Ag}_2\text{S}$  nanoparticles. The interplanar distance of the typical nanoparticle was  $2.66 \text{ \AA}$ , in accordance with that of (120) plane of monoclinic  $\text{Ag}_2\text{S}$  phase (JCPDS:14-0072). (d) The statistical diameter distribution histogram of  $\text{Ag}_2\text{S}$  nanoparticles. The dark curve was the fitted Gaussian plot.

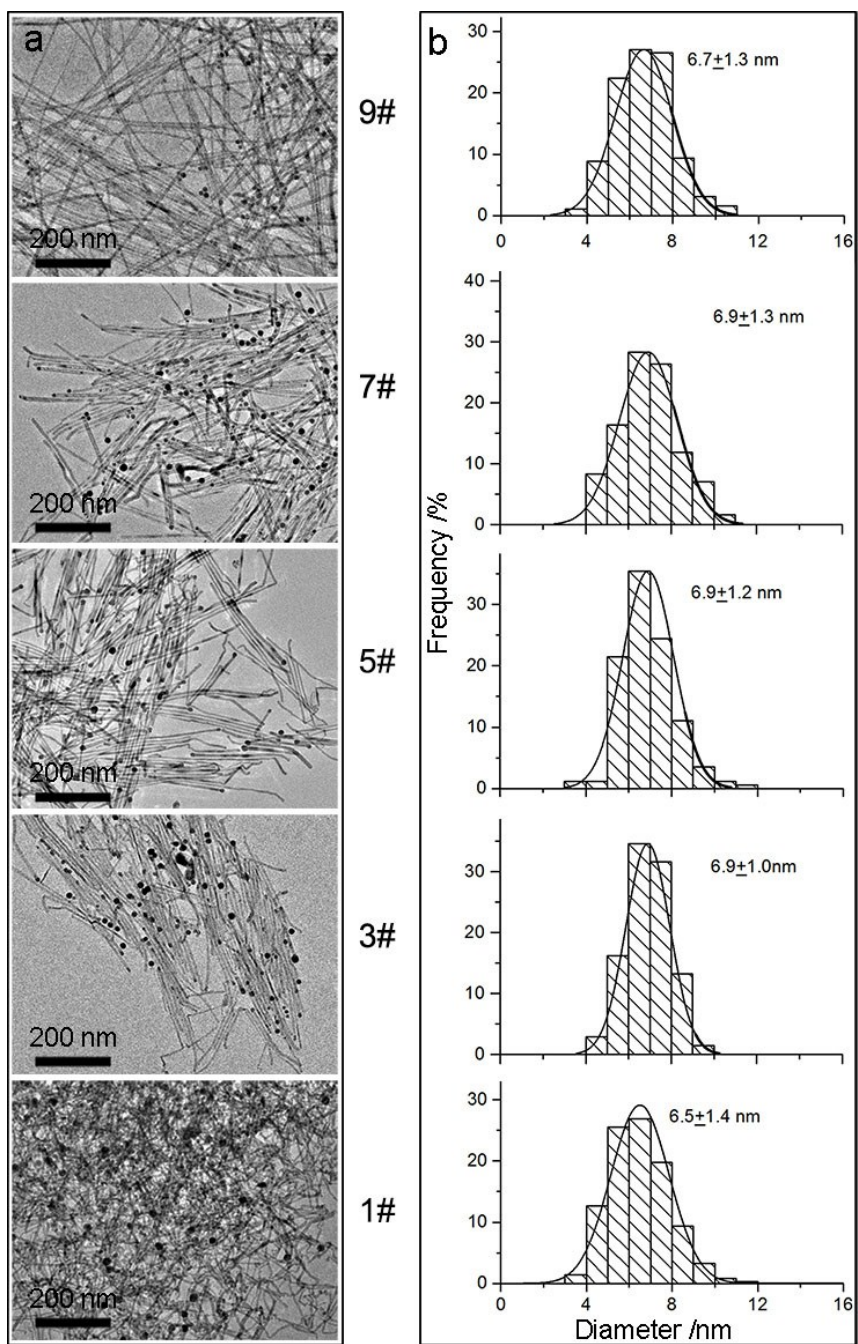


**Fig. S2** (a) TEM images of the samples 1, 3, 5, 7, 9#. (b) The diameter distributions of the nanowires of the five samples without consideration of the terminated nanoparticles. The dark lines were the corresponding fitted Gaussian plots.

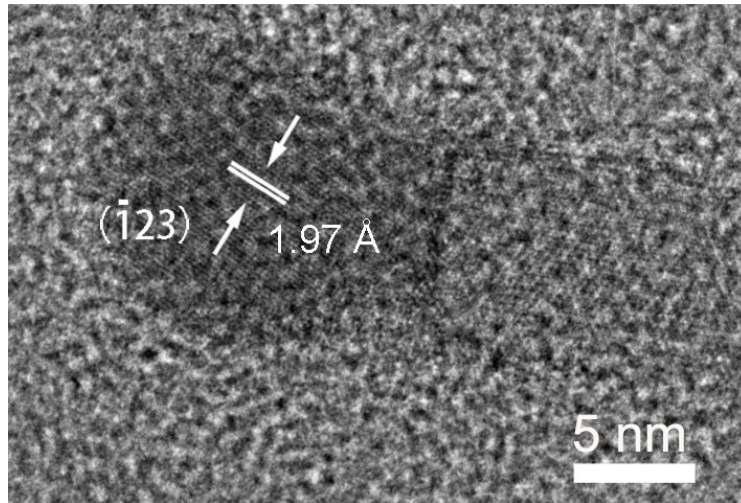


**Fig. S3** HRTEM image of terminated nanoparticle part of the same sample in Fig. 2d. The measured interplanar distance of the nanoparticle was 1.97 Å, in accordance with the spacing of (23) planes of monoclinic  $\text{Ag}_2\text{S}$  phase (JCPDS:14-0072).

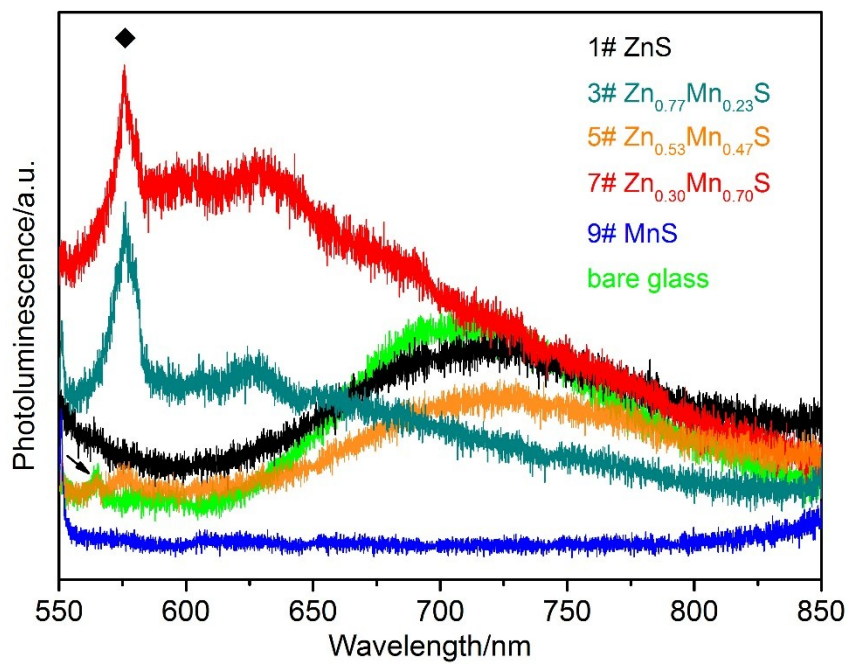


**Fig. S4** PL spectra of the typical samples 1, 3, 5, 7, 9# and bare glass. The 532 nm laser was used as the excitation source. The peaks denoted by the arrow came from the bare glass.

It can be seen that the samples 1# (ZnS) and 9# (MnS) show featureless PL spectra, however, the ternary  $\text{Zn}_{1-x}\text{Mn}_x\text{S}$  samples of 3, 5, 7# show clear characteristic yellow emission at 576 nm (denoted by ◆) from the  ${}^4\text{T}_1\text{-}{}^6\text{A}_1$  transition of  $\text{Mn}^{2+}$  dopant<sup>4</sup>, which indicates the formation of ternary alloyed  $\text{Zn}_{1-x}\text{Mn}_x\text{S}$  compound.

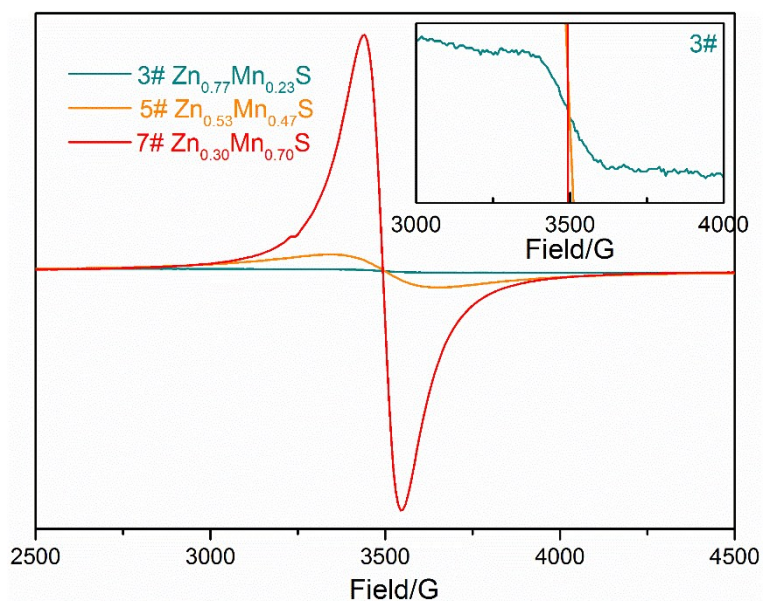


**Fig. S5** Room temperature X-band EPR spectra of the typical samples of 3, 5, 7#. Inset is the enlarged EPR spectrum of sample 3#.

The increased EPR intensity from samples 3# to 5# and 7# indicates the increased amount of  $\text{Mn}^{2+}$  in the  $\text{Zn}_{1-x}\text{Mn}_x\text{S}$  nanowires, and the hyperfine structure of  $\text{Mn}^{2+}$  cannot be resolved due to the high  $\text{Mn}^{2+}$  concentration for these samples. These features are similar to those reported in  $\text{Cd}_{1-x}\text{Mn}_x\text{Se}$  nanocrystals<sup>5</sup>.

#### References:

1. J. Akhtar, M. Afzaal, M. Banski, A. Podhorodecki, M. Syperek, J. Misiewicz, U. Bangert, S. J. O. Hardman, D. M. Graham, W. R. Flavell, D. J. Binks, S. Gardonio and P. O'Brien, *J. Am. Chem. Soc.*, 2011, **133**, 5602-5609.
2. F. J. Xu, B. Xue, F. D. Wang and A. G. Dong, *Chem. Mater.*, 2015, **27**, 1140-1146.
3. W. M. Haynes, *CRC Handbook of Chemistry and Physics*, 95th ed., CRC, Boca Raton, FL, 2014–2015.
4. S. L. Shen, Y. J. Zhang, Y. S. Liu, L. Peng, X. Y. Chen and Q. B. Wang, *Chem. Mater.*, 2012, **24**, 2407-2413.
5. C. J. Barrows, P. Chakraborty, L. M. Kornowske and D. R. Gamelin, *ACS Nano*, 2016, **10**, 910-918.